Egyptian Journal of Chemistry

http://ejchem.journals.ekb.eg/

In Vitro Antibacterial and Anticancer Applications of Chitosan Nanoparticles Loaded with Apis Mellifera Venom

Asmaa E. Amer[a*], Zienab E. Eldin[b, c], Saeed S. Elnemr[d] , Basma H. Amin[e]

[a] *Entomology Department, Faculty of Science, Ain Shams University, Cairo, Egypt*
[b] *Department of Material Science and Nanotechnology, Faculty of Postgraduate Studies for Advanced Sciences, Beni-Suef University, Beni-Suef, Egypt*
[c] *Center for Material Science Zewail City of Science and Technology, Giza, Egypt*
[d] *Faculty of Agriculture, Majoring in Biotechnology, Menoufia University, Menoufia, Egypt*
[e] *The Regional Center for Mycology and Biotechnology, Al-Azhar University, Cairo, Egypt*

Abstract

Bee venom (BV) is a substantial ingredient in secondary metabolic products from honeybees (*Apis mellifera* L.). Polymers and their varieties are emphasized in modern research for their obvious biological functions in medication. Chitosan nanoparticles (Chs-NPs) are among the anticipations for this approach, which are contingent upon the type of nanoparticles employed for therapeutic purposes. The main objective of this research is to substitute chemicals with environmentally friendly manufacturing and extraction of chitosan from exuviae of black soldier fly, *Hermetia illucens* L., prepare exuvial chitosan nanoparticles (Chs-NPs), testing the placing of nanoparticles with the honeybee, *Apis mellifera* venom (BV-placed NPs), and evaluate the antibacterial and anticancer activities of both BV, Chs-NPs, and BV-placed NPs. FTIR spectrum of BV, Chs-NPs and BV-placed NPs were illustrated showed the different functional groups of the tested compounds. Hydrodynamic size, Zeta potential and PDI of synthesized nanoparticles of Chs-NPs 270.6±5.0, +30.1± 3.3 and 0.199±0.02, while for BV-Chs-NPs were 380.4±15.0, +25.2±2.5 and 0.514±0.01. BV loaded Chs- NPs has the highest antibacterial impact versus *M. smegmatis* with inhibition zone of 28.0 ± 0.4 mm. Additionally, BV loaded Chs-NPs has the most promising antitumor impact versus A549 with IC_{50} =274.37±0.1 µg/ml with minimal cytotoxicity versus Vero cells CC_{50}=62.24± 0.2 µg/ml with notable microscopic alterations. Bee venom (BV) when enclosed in the Chs-NPs showed a promising antibacterial impact versus *Mycobacterium smegmatis* as well as antitumor action versus A549 with an acceptable harmful level to be implemented for forthcoming uses.

Keywords: Bee venom; Black soldier fly; nanoparticles; *Mycobacterium smegmatis*; antitumor activity

1. Introduction

Antibiotic-resistant bacterial strains have developed as a result of the abuse of antibiotics, making it more difficult to treat and eradicate their diseases [1]. In normally sensitive bacteria, antibiotics' effects on microbial communities may cause genomic or mutational alterations that provide germs the ability to endure and proliferate as antibiotic-resistant bacteria (ARB) [2]. The majority of commonly used antibiotics and chemotherapeutic drugs are inherently ineffective against mycobacteria [3]. *Mycobacterium smegmatis* (*M. smegmatis*) is some acid-fast bacilli of the fast-growing mycobacteria, and its infection should be taken into consideration for persons with persistent infections of the skin and soft tissues at the place of injection or surgery spot after aesthetic operations [4]. Cases of *M. smegmatis* infection in immunocompetent people are linked to injuries, ongoing central venous catheterization, and minor surgical procedures, and aesthetic operations [5]. *M. smegmatis* infection can spread in those with impaired immune systems, leading to bacteraemia and fatalities [6]. The prevalence and mortality rates of cancer are both rising quickly worldwide, making it an important trigger of death in most regions of the globe, including Europe, China, and the United States [7]. Natural discharges from insects and animals have shown promise as complementary treatments, in addition to the more well-known herbal and plant-derived medicines [7]. There have been reports of an antimicrobial effect from bee venom versus bacteria through creation of pores across their membranes, causing harm to them before rupture [8]. Additionally, it demonstrated anti-cancer action versus a number of cancer cell lines, including those from breast, liver, melanoma, and prostate [9–12]. Insects, such *Hermetia illucens* L., have developed humoral immune reaction that create

*Corresponding author e-mail: asmaaamer@sci.asu.edu.eg; (Asmaa E. Amer).
Receive Date: 05 April 2024, Revise Date: 22 June 2024, Accept Date: 26 July 2024
DOI: 10.21608/ejchem.2024.281740.9557

powerful antimicrobial peptides (AMPs) to defend them against pathogen insertion, and these AMPs are thought to be potent natural antibiotic candidates [13,14]. The utilization of nanotechnology in the majority of biomedical fields has dramatically boosted. This includes the use of nanomaterials as antimicrobial, and biocidal agents as well as the loading of nanomaterials with bioactive components to improve their strength, absorbability, use, and dissolution in the human body [15]. Chitosan is amino- polysaccharide produced from deacetylated chitin, has several useful properties (e.g., its biodegradability, nontoxicity, biocompatibility, and efficient bioactivities) [16]. The activities of chitosan promoted its use in biomedicine for common uses, such as medication delivery, tissue science, antimicrobial forms, anticancer therapy, and dressings for injuries [17]. Therefore, the current study's objectives were to produce exuvial chitosan nanoparticles (Chs-NPs), load them with bee venom (BV), assess their bioactivities to inhibit *M. smegmatis*, and highlight the possible application as anticancer agents.

2.Results

2.1. FTIR analysis

The FTIR spectra of chitosan prepared from exuviae of Black soldier fly, Chs-NPs, BV, and BV-Chs- NPs were illustrated in (**Fig.1**). In the chitosan prepared from exuviae of Black soldier fly a strong peak at approximately 3468 cm^{-1} is observed, corresponding to the collective effects of hydrogen bond and stretched O–H. Additionally, the N–H stretching arising from primary amines overlaps in this area. Other significant absorption peaks detected in chitosan extracted include: 1719 cm^{-1} (indicative of carbonyl (C=O) stretching in the secondary amide I band), peaks at 1519 cm^{-1} (associated with the amide II (N–H) bended vibration), and a peak at 1060 cm^{-1} (attributed to stretched C–O–C). As showed in (**Fig.1B**), some differences are noted compared to the FC spectrum. The peak at 3468 cm^{-1}, observed in chitosan extracted, appears wider in Chs-NPs with a magnified relative intensity, indicating an improvement in bonds of hydrogen. Moreover, the Chs-NPs spectrum exhibits a clear peak at 1180 cm^{-1}, which corresponds to P=O stretching, suggesting linkage with TPP. While the main peaks and bands in chitosan extracted spectrum also appear in the Chs-NPs spectrum, they have slight shifting to similar wavenumbers. In the BV spectrum, the peak seen in the absorbance region of 3250–3420 cm^{-1} corresponds to the free vibrations of N–H stretching. The FTIR spectrum of BV also displays an amide bands, namely amide I at 1677 cm^{-1}, amide II at 1569 cm^{-1}, and additional band at 1113 cm^{-1} indicating unsystematic coil conformation (**Fig. 1C**). In the FTIR spectrum of the BV-Chs-NPs (**Fig. 1D**), the absorbance peak of BV associated with N–H stretching at 3413 cm^{-1} is both smaller in intensity and appeared at 3442 cm^{-1}. Furthermore, the amide I band of BV, initially found at 1677 cm^{-1}, is shifted to a higher wavenumber, specifically 1697 cm^{-1}, in the BV-Chs-NPs.

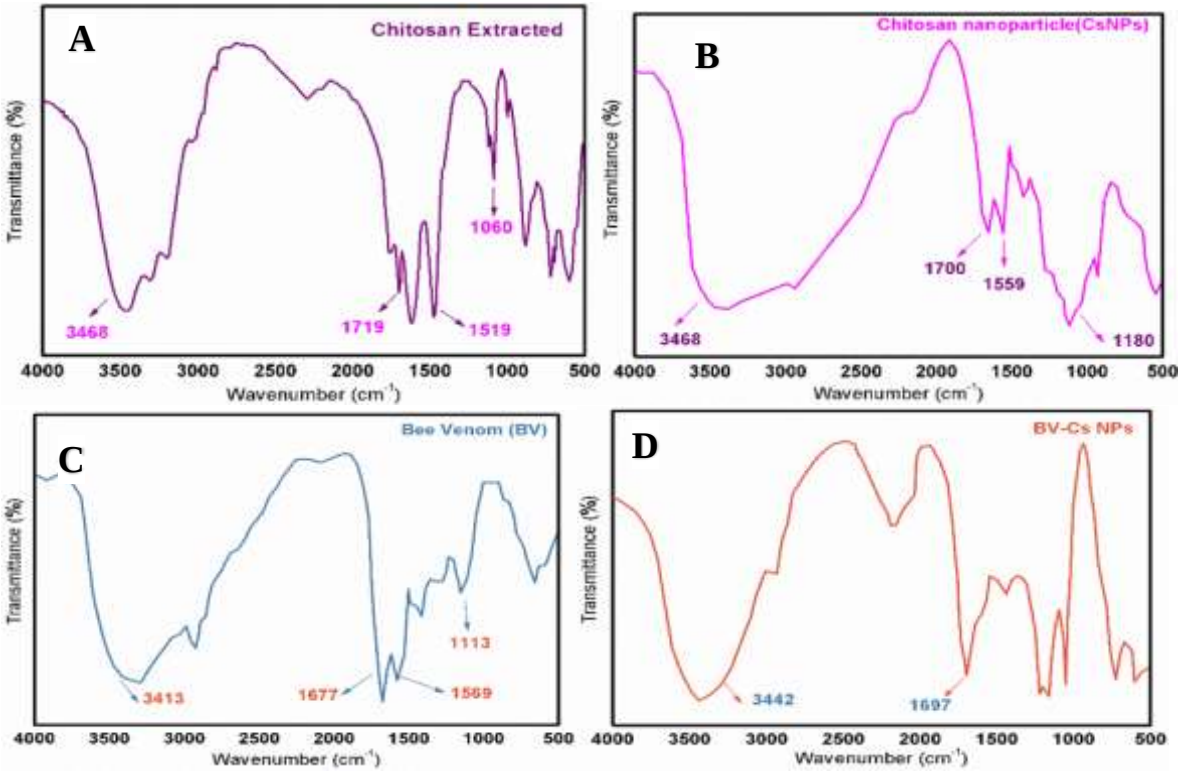

(Fig.1) Fourier-transform infrared spectroscopy spectra of **(A)** chitosan extracted from exuvia of black soldier fly, **(B)** chitosan nanoparticles, **(C)** bee venom, and **(D)** bee venom loaded chitosan nanoparticles.

2.2 Hydrodynamic size, Zeta potential, and Polydispersity index (PDI)

The hydrodynamic size, zeta potential and PDI of Chs- NPs and BV- Chs- NPs were illustrated in (**Table 1**). A reduction in the zeta potential was seen in BV-Chs- NPs compared to Chs-NPs. Additionally, a substantial boost in the PDI value was seen in BV-Chs-NPs relative to the Chs -NPs.

Table 1: The hydrodynamic size, Zeta potential and PDI of synthesized nanoparticles Chs-NPs and BV- Chs-NPs.

Nanoparticles	DLS (nm)	Zeta potential (mV)	PDI
Chs- NPs	**270.6±5.0**	**+30.1± 3.3**	**0.199±0.02**
BV-Chs- NPs	**380.4±15.0**	**+25.2±2.5**	**0.514±0.01**

2.3. TEM analysis

TEM examination was utilized to examine the particle size distribution and morphology of both Chs-NPs and BV-Chs-NPs as depicted in (**Fig.2**). The findings revealed that Chs-NPs had a mean size of 45.4± 10.55 nm and exhibited spherical shape with smooth surface. On the other hand, the BV-Chs-NPs displayed an average size of 115.75 ± 5.41 nm.

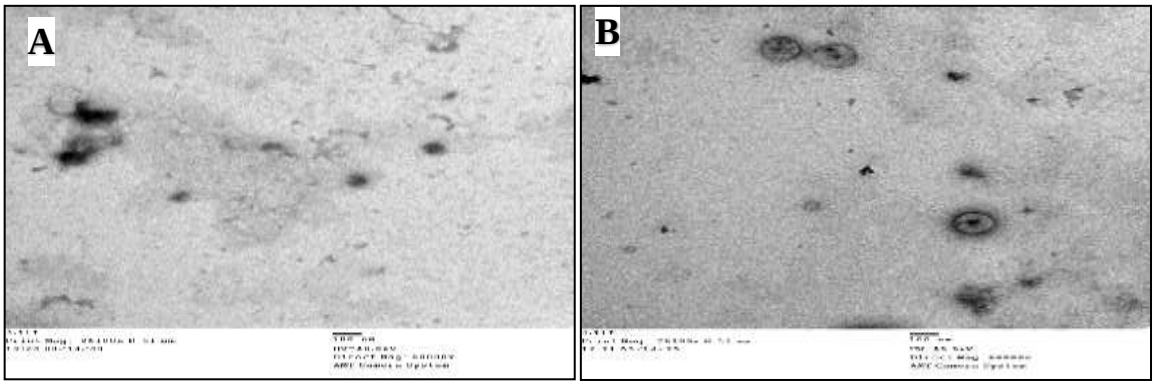

(Fig.2) Transmission electron microscope micrographs of(**A)**chitosan nanoparticles and (**B**) bee venom loaded chitosan nanoparticles (Magnification= 6000 ×).

2.4. Encapsulation efficiency (EE), Loading capacity (LC)

The EE and LC of BV in Chs-NPs were deemed to be 12.5% and 97.54%, respectively.

2.5. *In vitro* release of BV-Chs- NPs

To assess the release behaviour of BV from BV- Chs-NPs, *in vitro* detections were done at pH 7.3 by directly dispelled the specimens through a 24-hour release period. The BV release profile from BV-Chs-NPs is depicted in **(Fig.3)**. The release pattern demonstrated an initial burst release of BV within the first 5 hours, followed by a gradual release over the extended 24-hour period. Specifically, after 5 hours, 82.7% of BV was released. At the end of the 24-hour duration, the maximum release percentages reached 100%.

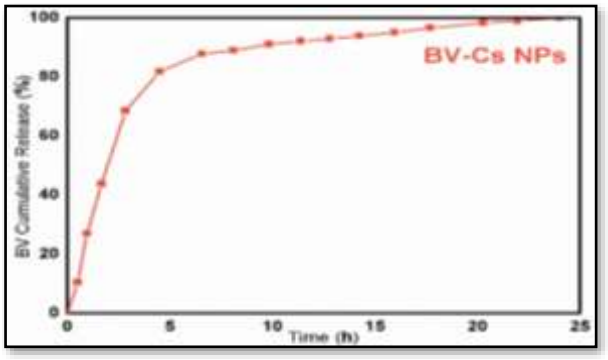

(Fig. 3) Bee venom release profile from bee venom loaded chitosan nanoparticles at different time intervals and pH 7.4.

2.6. *In vitro* Antibacterial role

All tested samples showed good antibacterial activity against *M. smegmatis*. BV showed inhibition zone of 12.0 ± 0.1 mm with MIC= 125 µg/ml, Chs-NPs had inhibition zone of 20.0 ± 0.3 and MIC= 62.5 µg/ml and BV loaded Chs-NPs showed inhibition zone of 28.0 ± 0.4mm with MIC = 125 µg/ml where the doxycycline (standard drug) had inhibition zone of 32.0 ± 0.4mm with MIC = 25.0± 0 µg/ml. Thus, the most effective was BV loaded Chs-NPs as seen in (**Fig. 4**).

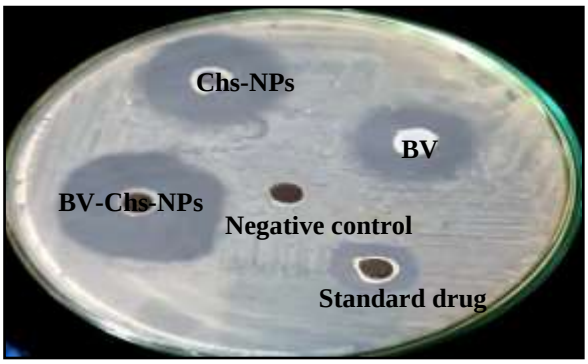

(Fig. 4) Antibacterial activity of negative control, bee venom (BV), chitosan nanoparticles (Chs-NPs), and bee venom loaded chitosan nanoparticles (BV-Chs-NPs) against *M. smegmatis*.

2.7. Cytotoxic activity on (A549) adenocarcinoma cells and normal Vero cells

A dose dependent cytotoxic impact for BV, Chs-NPs, and BV loaded Chs-NPs with IC_{50} values of 173.75±0.07 µg/ml, 231.9034 µg/ml and 274.37±0.1 µg/ml versus A549 respectively. In contrary the cytotoxicity against normal Vero cells CC_{50} values were 69.54±0.22 µg/ml, 70.68 ± 0.1 µg/ml and 62.24± 0.2 µg/ml respectively as depicted in (**Fig. 5**).

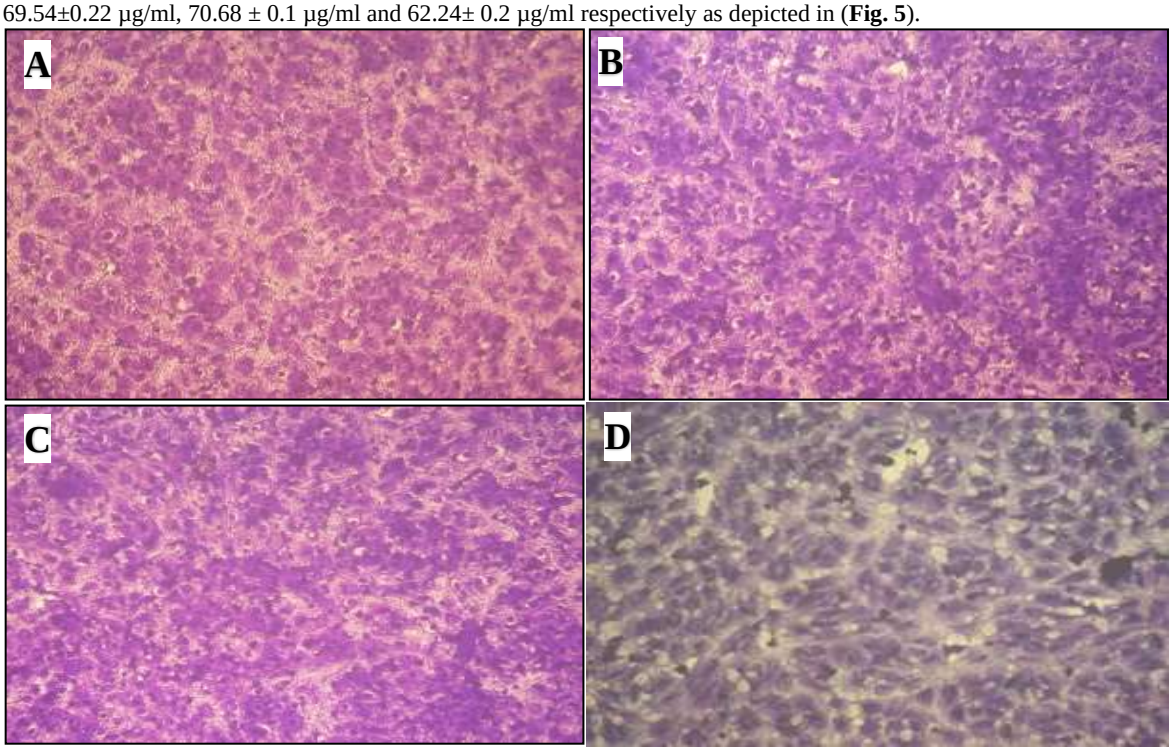

(Fig. 5) *In vitro* cytotoxic activity of **(B)** bee venom, **(C)** chitosan nanoparticles, **(D)**bee venom loaded chitosan nanoparticles against **(A)**normal Vero cells (Magnification = 100 ×).

2.8. Microscopic examination

Ultrastructural testing of the bacterial cells (*M. smegmatis)* using TEM: control cells showed intact membrane and elongated normal shape (**Fig. 6A).** While, upon treatment with BV cells showed alteration in cell structure and partial damage in cell membrane (**Fig.6B)**. Additionally, the treatment with Chs-NPs cells showed shrinkage of cytoplasmic fluid and irregular cell membrane (**Fig. 6C).** Finally, when BV loaded Chs-NPs was applied, the cells showed complete damage and deformation (**Fig. 6D).**

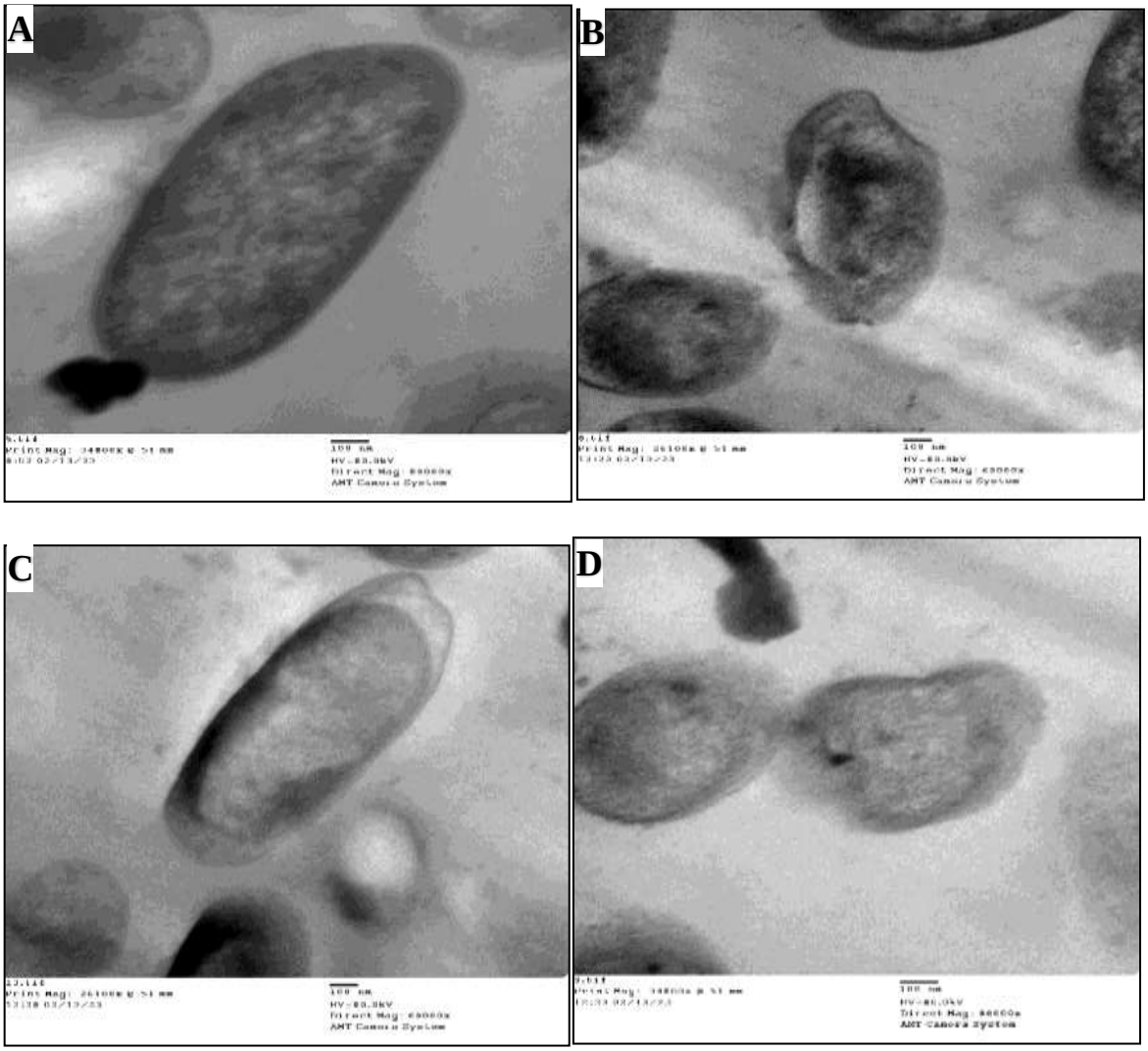

(Fig.6) Transmission electron microscope micrographs of *M. smegmatis*. **(A)** Control, **(B)** treated with bee venom, **(C)** treated with chitosan nanoparticles, and **(D)** treated with bee venom loaded chitosan nanoparticles (Magnification 6000 x).

Morphological alterations of A549 cells adenocarcinoma cells upon exposure using BV, Chs-NPs, and BV loaded Chs-NPs were seen under an inverted microscope. The stained cells indicated number of dead cells, the cells treated with BV represented morphological alterations including granulation, compression, and uneven form as defining characteristics **(Fig. 7B**). Besides, cells treated with Chs-NPs showed compression, aggregation of cells and distracted shape (Fig.7C). Lastly, cells treated with BV loaded Chs-NPs showed existence of dead bodies and a large vacuolation in the cell cytoplasm indicated autophagy-like process (**Fig. 7D)**.

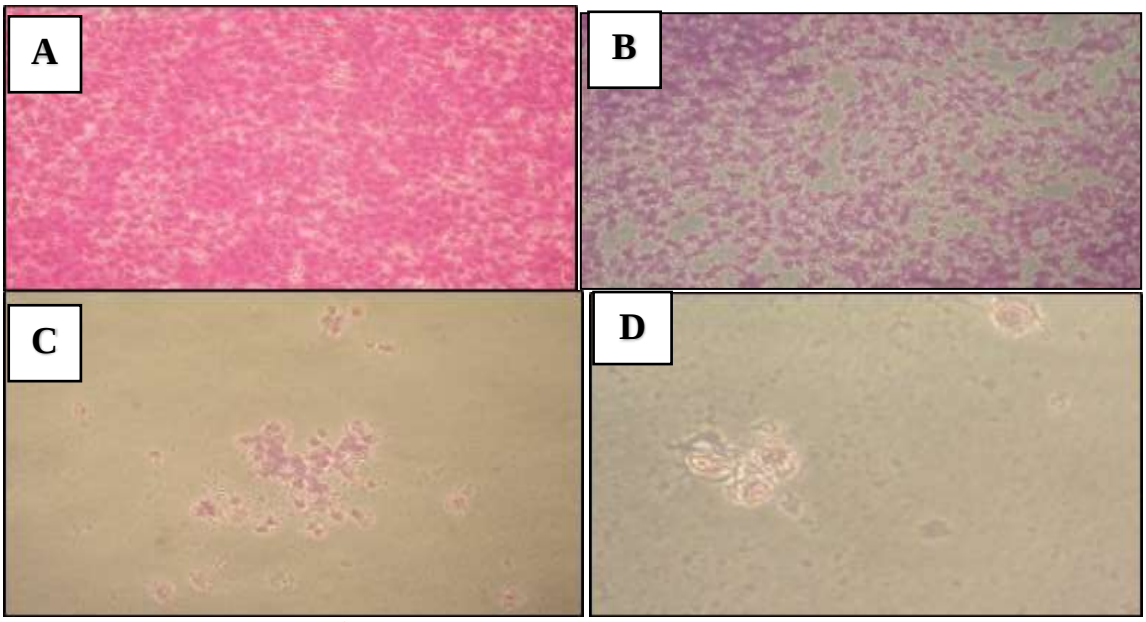

(Fig.7) Morphological characteristics of A549 cells adenocarcinoma cells using inverted microscope **(A)** Control, **(B)**treated with bee venom, (**C)** treated with chitosan nanoparticles, and (**D**) treated with bee venom loaded chitosan nanoparticles (Magnification 100 x).

Moreover, electron imaging revealed that the entire group of A549 cells, adenocarcinoma cells in the control group, are associated with numerous plasma cell membrane projections with numerous microvilli (**Fig. 8A**). However, following BV cell administration, apoptotic bodies and apoptotic cells were separated (**Fig. 8B**). Additionally, the Chs-NPs cell exposure resulted in a ruptured cell membrane and a constricted nucleus (**Fig. 8C**). Ultimately, following treatment with BV-loaded Chs-NPs, cells exhibited primary referral to apoptosis along with total lysis (**Fig. 8D**).

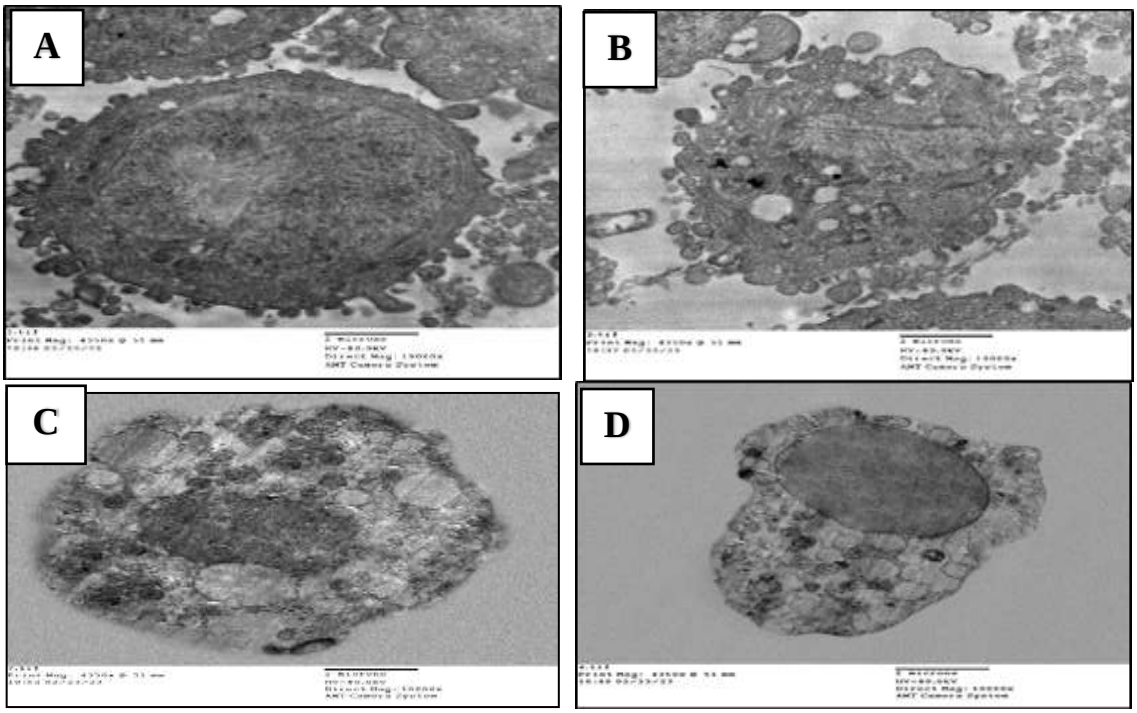

(Fig.8) TEM micrograph of the ultrastructural characteristics of A549 cells adenocarcinoma cells (**A**) control, (**B**) treated with bee venom, (**C**)treated with chitosan nanoparticles, and (**D**) treated with bee venom loaded chitosan nanoparticles (Magnification 10,000 X).

3.Discussion

Nanomedicine is a novel approach with a crucial function in both prevention and treatment of many diseases [18-21]. The original source of chitosan, crustacean waste, became no longer sustainable, On the alternative, the rearing of bio-converting insects, as well as the recycling of insect biomass, represent a waste stream of facilities that may be utilized for several applications [22].

In the present work a successful production of chitosan was accomplished using exuvia of black soldier fly. The black soldier fly - derived chitin and Chitosan were reported as novel sources for these valuable components [23]. This provided further confirmation of previous research indicating the considerable potential of these exuvia as sustainable sources for chitosan production [24-27]. These studies have suggested the utilization of chitosan derived from various chitin sources in biomedicine and drug delivery applications. The FTIR analysis of chitosan extracted demonstrated that its structure and functional groups closely resembled those of the standardized conventional chitosan [28]. Many distinctive peaks and bands in the chitosan obtained spectrum showed modest alterations that brought them nearer to the wavenumbers seen in the Chs-NPs spectrum, confirming the effectiveness of the Chs -NPs cross-linking and manufacture of the intended NPs. Moreover, comparing the Chs-NPs and BV-Chs-NPs spectra provided evidence of BV uptake by the nanoparticles. Specific bands characteristic of nanoparticles was observed in both spectra, indicating the presence of nanoparticles in both free BV and BV-Chs-NPs [1].

The data obtained from the "Zetasizer" analysis of the synthesized Chs-NPs and BV-Chs-NPs demonstrated that the BV-Chs nanoparticles had larger sizes compared to Chs-NPs. This increase in size can likely be attributed to the additional molecular weight and composite structure resulting from the incorporation of BV on Nano chitosan [29]. This result indicates the enhanced capacity of the current Chs-NPs to carry BV, making it a promising carrier for this bioactive compound. The TEM analysis has supported the hypothesis that BV was successfully incorporated into Chs-NPs. This was evident from the observed size difference among the BV-Chs-NPs and Chs-NPs. The liberation of BV from BV-Chs-NPs exhibited a rapid burst release during the initial 5 hours of the experiment. This sudden liberation is believed to be influenced by the detachment of BV molecules from the surface of Chs-NPs, a phenomenon commonly observed with loaded protein molecules on chitosan nanoparticles [30]. Following the initial burst release, the subsequent slow release of BV can be attributed to the gradual lysis of the entrapped protein molecules within Chs-NPs and the destruction of the nanoparticles themselves. It is hypothesized that the degradation rate of the protein exceeded its release rate after an extended period of release [31]. Besides, Khalil et al., [32] investigated that loading of bee venom on degradable polymers such as poly-D, L-lactic-co-glycolic acid (PLGA), and chitosan could improve its delivery and release. By employing such polymer NPs, bee venom may keep its releases and potency for an extended period of time, minimizing the time between injection and improving patient adherence [33, 34].

The use of *M. tuberculosis*, a slow-growing organism, made early attempts to screen TB medicines ineffective. *M. smegmatis* has gained recognition as an effective model organism for preliminary drug evaluation and additional drug optimization in more recent years due to the generalization of the majority anti-TB medicines among all mycobacteria [35]. Animal venom peptides, particularly BV, offer an enormous number of prospects for use as biological medicines. However, there are a lot of obstacles that could be removed by carrying the peptides onto polymeric nanocarriers such as Chs-NPs in order to increasing their stability, half-lives, oral absorption, and target cytotoxicity [36], this is assured by our study as the antibacterial activity of bee venom increased when its loaded in Chs-NPs with inhibition zone 28.0 ± 0.4 mm versus *M. smegmatis*. This result of the antibacterial activity is not contrasted with those reported by Sharaf et al. [37] Besides, Wehbe et al. [38] investigated that the crude BV have shown antitumor role towards different cancer cell types. our study also revealed the antitumor role of bee venom loaded on Chitosan nano particles against adenocarcinoma human alveolar cells. This finding corresponded well with the findings of Taher et al. [39], who reported that the bee venom–loaded nanoparticles had good anticancer properties.

4.Experimental

4.1 Chemicals and Bacteria

Sodium tri-poly phosphate (TPP), acetic acid, dimethyl sulfoxide (DMSO), and ethanol were obtained from Sigma (Sigma-Aldrich Co., CA, USA). The exuviae of *H. illucens* L. were obtained from (AMININS Co., for organic waste recycling, Cairo, Egypt) for recycling organic wastes. Honeybee venom was obtained from Department of honey bee researches, Institute of plant protection, Ministry of Agriculture, Dokki, Giza, Egypt. Every chemical and solvent utilized was of the highest grade and analytical quality. *M. smegmatis* (ATCC 700084) was kindly provided from Microbiology-department- Beni-Swief University.

4.2 Developing black soldier fly exuvia in powder form

Five g of fresh black soldier fly exuvia were meticulously cleaned with distilled water, roasted for 36 hours at 70 °C in an oven, ground in a mixer, and then kept at room temperature for additional testing.

4.3 Preparation of chitosan from black soldier fly exuvia

To obtain chitosan the following steps were done:

100 g of shells was placed in 0.06 M acetic acid for 25 hours. Then, after using distilled water to wash the specimens, they were then dried for Five hours at 75˚C in an oven. The result powder soaked in 12.5 M NaOH in (1:15 w/v) for 2 hours under magnetic stirrer, then cooling for 35 minutes at ambient temperature. After filtering the demineralized shells, the leftover material was cleaned with distilled water and dried again. To the result powder, one litre of 1% HCL was incorporated, and it

was allowed for 24 hours. Then, the mixture was centrifuged at 4000 rpm for 12 minutes, and the supernatant was disposed of. After being cleaned with distilled water, the remaining material was allowed to air out for four hours at 75˚C in an oven. Using a magnetic stirrer, a 50% NaOH solution (1:10 w/v) was added and heated to 100˚C for six hours. After cooling to ambient temperature, the specimen was filtered, cleaned with distilled water to achieve a pH of neutral, and then dried out at 75˚C in an oven. The ultimate product that was produced was chitosan [40].

4.4 Production of chitosan nanoparticles (Chs- NPs) and bee venom placed nanoparticles (BV-Chs- NPs)

Chitosan nanoparticles (Chs-NPs) were fabricated using the ionotropic gelation method [41].

0.32 g chitosan was mixed in 1.0 % of acetic acid, 100 ml of deionized water and mixed at regular temperature. Chitosan solution was raised to a pH of 5.0 using 1M NaOH. A 0.1 g of tripolyphosphate was dissolved in 33.3 ml of distilled water to prepare a sodium tripolyphosphate solution. Tripolyphosphate solution (TTP) was added to the chitosan solution with stirring at 1000 rpm, room temperature, in the ratio 3:1 (v/v) (chitosan: TPP), sonication was performed for 25 min. The obtained chitosan suspension was cooled, rotated at 12000 rpm for 60 minutes, then stored at 4 °C.

The process of obtaining bee venom-loaded nanoparticles involved adding 0.10 g of venom to the TPP solution prior to putting it to the chitosan solution. The combination was subsequently divided using a centrifuge set at 13000 rpm and 5°C for 60 minutes and kept at 4 °C for storage.

4.5 Examination of prepared black soldier fly chitosan, chitosan nanoparticles (Chs-NPs) and bee venom loaded nanoparticles (BV-Chs-NPs)

4.5.1. Fourier transform-infrared spectroscopy (FT-IR)

A compact FTIR spectrometer (Agilent Co., USA) was used to identify the chemical structures of the produced chitosan, Chs-NPs, BV, and BV-Chs-NPs. To create discs, the specimens were combined with spectroscopic-grade potassium bromide (KBr) and condensed. The produced materials' spectra were measured in spectral range between the 4000 and 500 cm^{-1}.

4.5.2. Evaluation of the particle size and zeta potential

The hydrodynamic size, zeta potential, and polydispersity index value have been computed with photon correlation spectroscope or dynamic light scattering (DLS) of the ZS92 Zeta sizer instrument (Malvern, United Kingdom) for Chs-NPs and BV-Chs-NPs.

4.5.3. Morphology study

The Chs-NPs and BV-Chs-NPs microstructure was investigated using a transmission electron microscope (TEM), a drop of the solution was applied to the copper grids covered with carbon and then left at the ambient temperature to dry. Transmission electron microscope (JEOL GEM-1010, Tokyo, Japan) at 80 kV at The Regional centre for Mycology and Biotechnology, (RCMB) Al- Azhar University was applied to characterize the specimens [42].

4.5.4. Detection of entrapment efficiency (EE) and loading capacity (LC)

The efficiency of bee venom entrapment was estimated by Bradford method, [43] which was calculated by deducting the entire amount of venom given to the nanoparticle formation solution from the quantity of venom that was not entrapped and left in the translucent supernatant. This was done after spinning for 65 minutes at 13000 rpm and 5°C, and the result was recorded at 595 nm. The estimation of free bee venom in the supernatant was conducted triply (n = 3), and a venom EE% and loading capacity (LC) was calculated.

4.5.5. *In Vitro* Release evaluation

Amount of 3 mg of BV-Chs-NPs was placed in Eppendorf tubes containing 3 ml of phosphate buffer (PBS), pH 7.2 under shaking. At certain time intervals (0.5, 1, 2, 3, to 24 hours), Samples was withdrawing and centrifuged at 11,000 rpm for 45 minutes.

The Bradford protein test is a spectrophotometric approach, which measures bee venom produced in the supernatant at 596 nm [44]. A standard curve was used to determine the total liberated levels of proteins at every interval [45].

4.6. Determination of Antibacterial Activity:

The antibacterial activity of BV, Chs-NPs and BV loaded Chs-NPs was investigated against *M. smegmatis* (ATCC 700084) using agar well diffusion method on nutrient agar media. The plates were left for 24 hours at 37°C, the inhibition zones were measured. The test was repeated three times. Various dilutions of the effective level were done and examined for *M. smegmatis* (ATCC 700084) to determine minimal inhibitory levels versus standard drug [46].

4.7. MTT Test and microscopic examination

The BV, Chs-NPs and BV loaded Chs-NPs were tested for cytotoxic effects on A549 adenocarcinoma human alveolar basal epithelial cells, and VERO cells. Following 24 hours of adhesion till confluence, specimens ranging in concentration from 500 to 15.63 µg/ml were added, and the cells were subsequently cultured for another 24 hours at 37°C. Following the addition of

the new medium, 100 µl of MTT solution (5 mg/ml) was added and let to sit for 4 hours at 37 °C. Using a microplate reader (Agilent Co, USA), absorbance was measured at 570 nm. IC_{50} the concentration needed to have a harmful impact on 50% of intact tumor cells is known as the 50% inhibitory level (IC_{50}). The level needed to have a harmful impact on 50% of healthy, undamaged cells is known as the cytotoxic concentration (CC_{50}). A digital camera and an inverted microscope (CZ43; Nikon, Japan) were used to take the pictures [45-47].

4.8. Electron microscopy

Mycobacterium smegmatis and A549 cells were treated with BV, Chs-NPs and BV loaded Chs-NPs and then fixed with 2.5% glutaraldehyde for 2 hours. The specimens were then immersed with 2.0% osmium tetroxide for 2.5 hours, and the blocks were dyed in 1.0% uranyl acetate and dehydrated with ascending levels of ethanol. The specimens were then put in resin, then cut by an ultra-microtome (Amos scientific, Germany), and the sections then investigated by a transmission electron microscope (JOEL, Japan) [48, 49].

4.9. Statistics

All examinations were done three times. A means with standard deviation (S.D) were recoded for each result.

5.Conclusions

The current work revealed that BV-loaded Chs-NPs have demonstrated comparatively superior outcomes compared to native BV and Chs-NPs alone. The *in-vitro* investigation demonstrated that BV-loaded Chs-NPs had a stronger antibacterial impact than the other options. Moreover, its cytotoxic impact was lower than that of solely native BV and Chs-NPs, and it will be confirmed by more sophisticated techniques. These results suggest that, with further research, BV-loaded Chs-NPs may prove to be a suitable substitute for antibiotics.

6. Compliance with ethical standards

This research paper was approved by the research ethics committee of IACUC of Beni-Suef University (BSU/FS/2024/1).

7.Conflicts of interest

"There are no conflicts to declare".

8.Formatting of funding sources

Non-applicable

9.Acknowledgments

Non-applicable

10. Abbreviations

M. smegmatis: Mycobacterium smegmatis
ARB: antibiotic-resistant bacteria
RGM: rapidly growing mycobacteria
AMPs: antimicrobial peptides
Chs-NPs: Chitosan nanoparticles
BV: bee venom
TEM**:** transmission electron microscope
TTP: Sodium tripolyphosphate solution
BV-Chs-NPs: Bee Venom loaded nanoparticles
EE: entrapment efficiency
LC: loading capacity
S.D: Standard deviation
PDI: Polydispersity index
M. tuberculosis: Mycobacterium tuberculosis
TB: Tuberculosis

11.References and Bibliography

[1] Sameh, A, Gouda AA, Elmligy E, Hatem H, Sadek SS, Ahmed O, El Amir A. (2023). Bee venom as an alternative for antibiotics against *Staphylococcus aureus* infections. *Scientific Reports* 13(1), 6436.

[2] Ben Y, Fu C, Hu M, Liu L, Wong MH, Zheng C (2019). Human health risk assessment of antibiotic resistance associated with antibiotic residues in the environment: A review. *Environmental research*, 169, 483-493.

[3] Ren H., Liu, J. (2006). AsnB is involved in natural resistance of *Mycobacterium smegmatis* to multiple drugs. *Antimicrobial agents and chemotherapy*, 50(1), 250-255.

[4] Wang CJ, Song Y, Li T, Hu J, Chen X., Li, H (2022). *Mycobacterium smegmatis* skin infection following cosmetic procedures: report of two cases. Clinical, *Cosmetic and Investigational Dermatology*, 535-540.

[5] Butt S, Tirmizi A (2019). *Mycobacterium smegmatis* bacteremia in an immunocompetent host. ID Cases, 15, e00523.

[6] Pierre-Audigier C, Jouanguy E, Lamhamedi S, Altare F, Rauzier J, Vincent V, Canioni D, Emile JF, Fischer A, Blanche S, Gaillard JL, Casanova JL. (1997). Fatal disseminated *Mycobacterium smegmatis* infection in a child with inherited interferon γ receptor deficiency. Clinical infectious diseases, 24(5), 982-984.

[7] Amin BH, Amer A, Azzam M, Abd El-Sattar NE, Mahmoud D, Al-Ashaal S, Areej A. Al-Khalaf, Hozzein WN (2022). Antimicrobial and anticancer activities of *Periplaneta americana* tissue lysate: An in vitro study. Journal of King Saud University-Science, 34(5), 102095.

[8] Wehbe R, Frangieh J, Rima M, El Obeid D, Sabatier JM, Fajloun, Z (2019). Bee venom: Overview of main compounds and bioactivities for therapeutic interests. Molecules, 24(16), 2997.

[9] Liu, X., Chen, D., Xie, L., & Zhang, R. (2002). Effect of honey bee venom on proliferation of K1735M2 mouse melanoma cells in-vitro and growth of murine B16 melanomas in-vivo. *Journal of pharmacy and pharmacology*, *54*(8), 1083-1089.

[10] Seidenberg DM, Baptista-Saidemberg NB, Palma MS (2011). Chemometric analysis of Hymenoptera toxins and defensins: A model for predicting the biological activity of novel peptides from venoms and hemolymph. Peptides. 32, 1924–1933.

[11] Jung GB, Huh JE, Lee HJ, Kim D, Lee GJ, Park HK, Lee JD (2018). Anti-cancer effect of bee venom on human MDA-MB- 231 breast cancer cells using Raman spectroscopy. Biomed. Opt. Express, 9, 5703–5718.

[12] Hong J, Lu X, Deng Z, Xiao S, Yuan B, Yang X (2019). How Melittin inserts into cell membrane: Conformational changes, interpeptide cooperation, and disturbance on the membrane. Molecules, 24, 1775.

[13] Kalsy M, Tonk M, Hardt M, Dobrindt U, Zdybicka-Barabas A, Cytrynska, M, Vilcinskas, A, Mukherjee K (2020). The insect antimicrobial peptide cecropin A disrupts uropathogenic *Escherichia coli* biofilms. NPJ Biofilm. Microbiomes, 6, 1–8.

[14] Wu Q, Patoˇcka, J, Kuˇca K (2018). Insect antimicrobial peptides, a mini review. Toxins, 10, 461.

[15] Sahoo SK, Parveen S, Panda JJ. (2007). The present and future of nanotechnology in human health care. Nanomedicine: Nanotechnology, Biology and Medicine, 3, 1, pp. 20–31.

[16] Rabea EI, Badawy ME, Stevens CV, Smagghe G, Steurbaut W (2003). Chitosan as antimicrobial agent: applications and mode of action. *Biomacromolecules*, 4, 6: 1457–1465.

[17] Felt O, Buri P, Gurny R (1998). Chitosan: a unique polysaccharide for drug delivery. *Drug Development and Industrial Pharmacy*. 24, 11: 979–993.

[18] de Queiroz Antonino RSCM, Lia Fook BRP, de Oliveira Lima VA, de Farias Rached RÍ, Lima EPN, da Silva Lima RJ, Peniche Covas CA, Lia Fook MV. (2017). Preparation and characterization of chitosan obtained from shells of shrimp (*Litopenaeus vannamei* Boone). *Marine drugs*, 15(5), 141.

[9] Elnosary ME, Aboelmagd HA, Habaka MA, Salem SR, El-Naggar ME (2023). Synthesis of bee venom loaded chitosan nanoparticles for anti-MERS-COV and multi-drug resistance bacteria. Int J Biol Macromol.;224:871-880.

[20] El-Mongy, A., Imam, A. A., & Othman, A. S. (2023). In Vitro Effect of Chitosan *Lactobacillus acidophilus* Nanoparticles On Vancomycin-Resistant Multidrug-Resistant *Enterococcus faecalis*. *Egyptian Journal of Chemistry*, *66*(13), 797-805.

[21] El-Enain, A., Abed, N., Abu Senna, A. S., Abdelkhalek, E., Safwat, N. A., & Yosri, M. (2024). In vitro testing of biomedical applications of biosynthesized titanium nanoparticles using *Saccharopolyspora spinosa*. *Egyptian Journal of Chemistry*, *67*(5), 109-125.

[22] Ali, O. A. M., Abou-Taleb, K. A., Elbauomy, E. M., & Abd Elhady, H. M. (2022). Antibiotics Immobilized Gelatin Nano Carrier Influences on *Brucella melitensis* Filed Strain. *Egyptian Journal of Chemistry*, *65*(132), 245-254.

[23] Essa, E. E., Hamza, D., Khalil, M. M., Zaher, H., Salah, D., Alnemari, A. M., & Momen, S. A. (2022). The antibacterial activity of Egyptian wasp chitosan-based nanoparticles against important antibiotic-resistant pathogens. *Molecules*, *27*(21), 7189.

[24] Khayrova, A., Lopatin, S., & Varlamov, V. (2019). Black soldier fly *Hermetia illucens* as a novel source of chitin and chitosan. *Int. J. Sci*, *8*(04), 81-86.

[25] Hahn T, Tafi E, Paul A, Salvia R, Falabella P, Zibek, S. (2020). Current state of chitin purification and chitosan production from insects. Journal of Chemical Technology & Biotechnology, 95(11), 2775-2795.

[26] Lin, Yin-Shen, Shih-Hsiang Liang, Wen-Lin Lai, Ja-Xin Lee, Ya-Peng Wang, Yi-Tsz Liu, Szu-Han Wang, Meng-Hwan Lee. (2021). Sustainable extraction of chitin from spent pupal shell of black soldier fly. Processes, 9(6), 976.

[27] Ma J, Faqir Y, Tan C, Khaliq, G. (2022). Terrestrial insects as a promising source of chitosan and recent developments in its application for various industries. Food Chemistry, 373, 131407.

[28] Rehman Ku, Hollah C, Wiesotzki K, Heinz V, Aganovic K, Rehman Ru, Petrusan J-I, Zheng L, Zhang J, Sohail S, Mansoor MK, Rumbos CI, Athanassiou C, Cai, M. (2023). Insect-derived chitin and chitosan: A still unexploited resource for the edible insect sector. Sustainability, 15(6), 4864.

[29] Soares KSR, Fonseca JLC, Bitencourt MAO, Santos KS, Silva-Júnior AA, Fernandes-Pedrosa, MF (2012). Serum production against *Tityus serrulatus* scorpion venom using cross-linked chitosan nanoparticles as immunoadjuvant. Toxicon, 60(8), 1349-1354.

[30] Jarudilokkul S,Tongthammachat A,Boonamnuayvittaya V (2011). Preparation of chitosan nanoparticles for encapsulation and release of protein. Korean Journal of Chemical Engineering, 28, 1247-1251.

[31] Xu Y, Du Y (2003). Effect of molecular structure of chitosan on protein delivery properties of chitosan nanoparticles. International journal of pharmaceutics, 250(1), 215-226.

[32] Khalil, A., Elesawy, B. H., Ali, T. M., & Ahmed, O. M. (2021). Bee venom: From venom to drug. Molecules, 26(16), 4941.

[33] Park MH, Kim JH, Jeon JW, Park JK, Lee BJ, Suh GH, Cho CW (2015). Preformulation Studies of Bee Venom for the Preparation of Bee Venom-Loaded PLGA Particles. Molecules, 20, 15072–15083.

[34] Alalawy AI, El Rabey HA, Almutairi FM, Tayel AA, Al-Duais MA, Zidan NS, Sakran I (2020). Effectual Anticancer Potentiality of Loaded Bee Venom onto Fungal Chitosan Nanoparticles. Int. J. Polym. Sci. 2020, 2785304.

[35] Sparks IL, Derbyshire KM, Jacobs WR Jr, Morita YS. *Mycobacterium smegmatis*: The Vanguard of Mycobacterial Research. J Bacteriol. 2023 Jan 26;205(1): e0033722.

[36] Dos Santos AP, de Araújo TG, Rádis-Baptista G. (2020). Nanoparticles functionalized with venom-derived peptides and toxins for pharmaceutical applications. Current Pharmaceutical Biotechnology, 21(2), 97-109.

[37] Sharaf, M., Zahra, A. A., Alharbi, M., Mekky, A. E., Shehata, A. M., Alkhudhayri, A., ... & Liu, C. G. (2024). Bee chitosan nanoparticles loaded with apitoxin as a novel approach to eradication of common
human bacterial, fungal pathogens and treating cancer. Frontiers in Microbiology, 15, 1345478.

[38] Wehbe R, Frangieh J, Rima M, El Obeid D, Sabatier JM, Fajloun Z (2019). Bee venom: Overview of main compounds and bioactivities for therapeutic interests. Molecules, 24(16), 2997.

[39] Taher, F. A., Moselhy, W. A., Mohamed, A. F., Didamony, S. E., Metwalley, K. M., & Zayed, A. B. (2017). Preparation and characterization of shrimp derived chitosan and valuation of its efficiency as bee venom delivery for cancer treatment. *Int. J. Adv. Res*, *5*(5), 370-388.

[40] El-Sherbiny MM, Elekhtiar RS, El-Hefnawy ME, Mahrous H, Alhayyani S, Al-Goul ST, Orif MI, Tayel AA (2022). Fabrication and assessment of potent anticancer nanoconjugates from chitosan nanoparticles, curcumin, and eugenol. *Front Bioeng Biotechnol*.;10:1030936.

[41] Amin BH, Ahmed HY, El Gazzar EM, Badawy MM (2021). Enhancement the mycosynthesis of selenium nanoparticles by using gamma radiation. *Dose-Response*, 19(4), 15593258211059323.

[42] El-Didamony, S. E., Amer, R. I., & El-Osaily, G. H. (2022). Formulation, characterization and cellular toxicity assessment of a novel bee-venom microsphere in prostate cancer treatment. *Scientific Reports*, *12*(1), 13213.

[43] Liu Y, Jin J, Xu H, Wang C, Yang Y, Zhao Y, Han H, Hou T, Yang G, Zhang L, Wang Y, Zhang W, Liang Q. (2021). Construction of a pH-responsive, ultralow-dose triptolide nanomedicine for safe rheumatoid arthritis therapy. *Acta Biomaterialia*, 121, 541-553.

[44] Jarudilokkul S, Tongthammachat A, Boonamnuayvittaya V (2011). Preparation of chitosan nanoparticles for encapsulation and release of protein. *Korean Journal of Chemical Engineering*, 28, 1247-1251.

[45] Amin B (2016). Isolation and characterization of antiprotozoal and antimicrobial metabolite from *Penicillium roqueforti*. Afr. J. Mycol. Biotech, 21, 13-26.

[46] Francis D, Rita L (1986). Rapid colorimetric assay for cell growth and survival: modifications to the tetrazolium dye procedure giving improved sensitivity and reliability. J. Immunol Methods 89: 271–277.

[47] Ke H, Hisayoshi K, Aijun D, Yonngkui J, Shigeo I, Xinsheng Y (1999). Antineoplastic agents-III: Steroidal glycosides from *Solanum nigrum.* Planta Med 65: 35–38.

[48] Elaasser MM, Abdel-Aziz MM, El-Kassas RA (2011). Antioxidant, antimicrobial, antiviral and antitumor activities of pyranone derivative obtained from *Aspergillus candidus*. J. Microbiol. Biotech. Res, 1(4), 5- 17.

[49] Amin BH, Abou-Dobara MI, Diab MA, Gomaa EA, El-Mogazy MA, El-Sonbati AZ, EL-Ghareib MS, Hussien MA, Salama HM (2020). Synthesis, characterization, and biological investigation of new mixed-ligand complexes. Applied Organometallic Chemistry, 34(8), e5689.